PHYSICAL REVIEW B **69**, 041307(R) (2004)

Phonon sidebands in exciton and biexciton emission from single GaAs quantum dots

E. Peter,[1] J. Hours,[1] P. Senellart,[1,*] A. Vasanelli,[1] A. Cavanna,[1] J. Bloch,[1] and J. M. Gérard[2]
[1]*CNRS-Laboratoire de Photonique et Nanostructures, Route de Nozay, 91460 Marcoussis, France*
[2]*CEA/DRFMC/SP2M, Nanophysics and Semiconductors Laboratory, 17, rue des Martyrs, 38054 Grenoble Cedex, France*
(Received 24 October 2003; published 26 January 2004)

We report on the observation of asymmetric phonon sidebands on both the exciton and biexciton emission lines in single GaAs monolayer fluctuation quantum dots. The contribution of phonon sidebands to the emission line is larger for the biexciton than for the exciton. We model the exciton line shape by means of a nonperturbative coupling with acoustic phonons and show that energetic confinement is an important clue to understand why phonon sidebands are sometimes observed and sometimes not. Finally, we discuss the extension of our model to the biexciton case.

DOI: 10.1103/PhysRevB.69.041307 PACS number(s): 78.67.Hc, 63.20.Ls, 71.35.Cc, 78.55.Cr

Semiconductor quantum dots (QD's) behave in many aspects similar to atoms with a spectrum which can be to a large extent artificially designed. Due to their reduced dimensionality, usual solid-state decoherence processes are expected to be inefficient so that QD's attract much interest in solid-state quantum optics and qubit generation.[1] QD's formed at an interface fluctuation of a quantum well are particularly attractive structures to this extent: they are expected to present a much larger oscillator strength than self-assembled QD's.[2] This makes them very good candidates for observing exciton-photon strong-coupling regime[2] or delivering Fourier transform limited single photons.[3] We have recently demonstrated that single-photon emission can be triggered from a single GaAs monolayer fluctuation QD.[4] Moreover, exciton and biexciton coherent control on monolayer fluctuation QD's has recently been demonstrated,[5,6] enabling the realization of an all-optical quantum gate.[6]

In solid-state physics, carrier-phonon interaction is an important cause for loss of coherence. However, in QD's, as the discrete excitonic states are separated by several meV, the interaction with phonons was expected to be drastically reduced. This led to the theoretical prediction of a phonon-relaxation bottleneck[7] and suggested that the QD dephasing time would only be limited by the radiative lifetime at low temperatures.[8] These ideas have stimulated considerable interest in investigating the homogeneous spectral linewidth of QD's.[8–11] Even if radiative limited linewidths of the order of few tens of μeV have been reported,[8,10] most of the time, a larger broadening is observed which is not fully understood. Several theoretical and experimental investigations have recently shown that the degrees of freedom for the lattice and exciton may no longer be treated separately. Indeed, strong-coupling regime between electrons and optical phonons has been demonstrated in InAs self-assembled QD's.[12] Moreover, a nonperturbative regime between acoustic phonons and excitons has been evidenced in II-VI QD's (Ref. 13) and nanocrystals[14] appearing as sidebands in the line profile.

In this paper, we report on the observation of a non-Lorentzian asymmetric broadening of both biexciton and exciton emission lines in GaAs monolayer fluctuation quantum dots. We show that these sidebands are due to a nonperturbative coupling to acoustic phonons. To our knowledge, it is the first observation of this nonperturbative regime for the biexciton: we observe that this coupling with acoustic phonons is even more important than in the exciton case. Moreover, phonon sidebands on the exciton line have never been reported on monolayer fluctuation QD's. We extend the Huang-Rhys model describing the coupling between acoustic phonons and electrons to the case of an exciton localized in a monolayer fluctuation QD. The calculated line shapes are in perfect agreement with experimental ones for various QD's, with different confinement energies and for different temperatures. The only parameter of the model is the QD lateral size, which we deduce from microphotoluminescence excitation (μ-PLE) measurements. We then discuss the extension of our model to the biexciton.

The investigated sample consists of a nominally 10-monolayer GaAs quantum well embedded in $Al_{0.33}Ga_{0.67}As$ barriers. The detailed description of the sample growth and its optical characterization can be found in Ref. 4. To perform single QD photoluminescence spectroscopy and increase the collected signal, QD's are isolated in microdisk structures with diameter around 2 μm. The sample is placed in a cold-finger helium flow cryostat which allows to vary the temperature between 5 K and room temperature. Microphotoluminescence (μ-PL) measurements were performed in the far field using a microscope objective (numerical aperture 0.4). The nonresonant excitation beam (a tunable cw Ti:sapphire laser with excitation energy around 1.75 eV) is focused on the sample with a spot size of about 2 μm. The same low excitation power ($\approx$30 W/cm^2) is used for all QD's in order to avoid heating by laser irradiation. The emission, collected by the same objective, is dispersed by a double grating spectrometer. The signal is detected either by a N_2-cooled Si charged-coupled device camera for μ-PL or by a low-noise Si photodiode for μ-PLE. The spectral resolution is 90 μeV.

We study the photoluminescence emission from two QD's, namely, QD1 and QD2, presenting different confinement energies, as we discuss hereafter. The emission of both QD's gives evidence for a biexcitonic state, which we identify by power dependent measurements. Further confirmation of the assignment of this emission line to a biexciton state has been checked in time-resolved μ-PL measurements:[15] the exciton emission line rises *after* the biexciton emission decays as in Ref. 16. For the excitation power used in these measurements ($\approx$30 W/cm^2), the biexciton line is hardly visible for QD1 whereas it clearly appears for QD2. Figure 1 shows the μ-PL spectra (thick lines) of QD1 and QD2 for

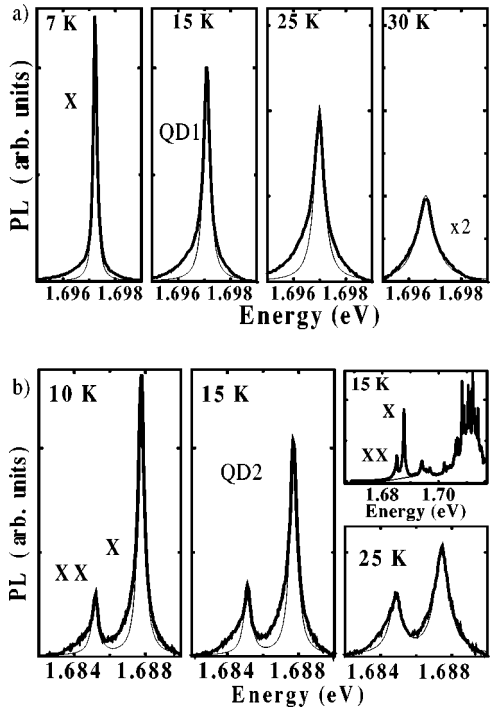

FIG. 1. μ-PL spectra (thick lines) from QD1 [upper part (a)] and QD2 [lower part (b)] for various temperatures and for an excitation power density $P=30\ \mathrm{W\,cm^{-2}}$. The thin lines represent Lorentzian profiles. The right upper part of (b) shows a broad energy window for QD2 at 15 K. A small background signal appears at the QD emission energy which we subtract locally as a straight line. Small background substraction has been done similarly for all spectra presented here.

various temperatures. At low temperature (7–15 K), exciton (QD1 and QD2) and biexciton (QD2) μ-PL line shapes deviate strongly from a Lorentzian line (thin lines in Fig. 1): a broad background appears on both sides of the central line with a larger intensity on the low-energy side. When increasing the temperature, the emission peaks show a redshift and a quenching of their intensity. Simultaneously, the exciton line becomes more symmetric, and displays a Lorentzian profile around 30 K. As shown in Fig. 2, the full width at half maximum (FWHM) of the luminescence lines increases with temperature following a two-step behavior for both exciton and biexciton. Actually, low-temperature values of FWHM correspond to the central line. At higher temperature (from 25 K for QD1 and from 15 K for QD2), the measured linewidth includes the sidebands and increases much more abruptly. At all temperatures the exciton line is broader for QD2 than for QD1.

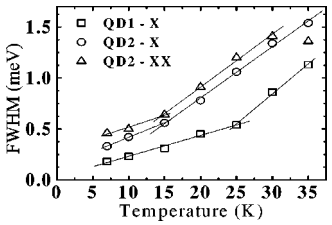

FIG. 2. Symbols: FWHM of exciton and biexciton emission lines for QD1 and QD2 as a function of temperature. The thin lines are linear fits.

From Fig. 1(b), we can note that the intensity ratio [(sidebands)/(central line)] at a given temperature is larger for the biexciton than for the exciton, indicating a stronger coupling to acoustic phonons. This is confirmed considering Fig. 2, where the temperature broadening of the biexciton line is larger than for the exciton line at all temperatures.

Phonon sidebands in single quantum dot are attributed to a nonperturbative coupling of excitons with acoustic phonons.[13] Following Ref. 13, we extend the Huang-Rhys theory of localized electron-phonon interaction to the case of an exciton confined in a monolayer fluctuation QD.[17] The exciton-phonon coupling Hamiltonian is written as $H_{X\text{-}ph}=c^{\dagger}c\Sigma_{\mathbf{q}}M_{\mathbf{q}}(b_{\mathbf{q}}^{\dagger}+b_{\mathbf{q}})$ where $c^{\dagger}$ and $b_{\mathbf{q}}^{\dagger}$ (respectively c and $b_{\mathbf{q}}$) are the creation (respectively annihilation) operators of an exciton with energy E_0 and a phonon with momentum $\mathbf{q}$ and energy $\hbar\omega_{\mathbf{q}}$. $M_{\mathbf{q}}$ is the coupling matrix element between excitons and phonons. This nonperturbative coupling gives rise to a *continuum* of mixed exciton-phonon states, which radiatively recombine. The central line of the emission is then called the zero-phonon line, and is surrounded by a continuum of one-phonon, two-phonon, . . . , p-phonon lines.

To quantitatively calculate this coupling for our QD's, we only consider the deformation potential due to the longitudinal acoustic (LA) phonon modes.[18,19] We consider an isotropic Debye dispersion relation for the LA phonon mode $\omega=u_s q$ (with an angular averaged sound velocity u_s of the LA mode.[17]) Thus, we take $M_{\mathbf{q}}=\sqrt{(\hbar q/2\rho u_s V)}(D_c\langle X|e^{i\mathbf{q}\cdot\mathbf{r_e}}|X\rangle - D_v\langle X|e^{i\mathbf{q}\cdot\mathbf{r_h}}|X\rangle)$, where D_c and D_v are the deformation potential of the conduction and valence bands, ρ the mass density, and V the quantization volume. For all calculations presented here, we take $D_v=5.6$ eV (Ref. 21) and $D_c=-11.5$ eV (Ref. 22).

In monolayer fluctuation quantum dots, the electron-hole Coulombic attraction is larger than the lateral confinement potential. Therefore, we consider a quasi-two-dimensional exciton, whose center of mass is weakly localized at the interface fluctuation of the quantum well. We write the wave function of the localized exciton state $|X\rangle$ as follows: $\psi_X(r_e,r_h)\propto e^{-R_{xy}^2/2\xi^2}e^{-\rho/\lambda}\cos(\pi z_e/L_z)\cos(\pi z_h/L_z)$, where R_{xy} is the center-of-mass position and ρ describes the electron-hole relative motion. ξ is a variational parameter describing the lateral extension of the center-of-mass movement in the QD.[18] $\lambda=6$ nm is the exciton Bohr radius for a 30 Å $GaAs/Al_{0.3}Ga_{0.7}As$ quantum well.[23]

To estimate the lateral size of the QD's and deduce ξ, we consider μ-PLE spectra shown in Fig. 3. Neither QD1 nor QD2 presents an excited state, indicating rather small QD sizes. The energy difference between the exciton line and the 2D absorption from the quantum well is $E_1=12$ meV for QD1 ($E_2=6.4$ meV for QD2). Macrophotoluminescence measurements show the energy difference between the emission of an n-monolayer and an $(n+1)$-monolayer quantum well.[4] This energy difference remains constant at different points of the sample, so that we can deduce the energy depth V_b of the 1-monolayer quantum well fluctuation.[24] We mea-

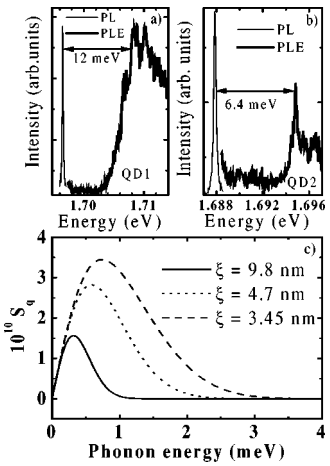

FIG. 3. Upper part: μ-PLE spectra for QD1 (a) and QD2 (b). Lower part (c): Huang-Rhuys factor S_q as a function of the phonon energy for three localization lengths ξ.

sure $V_b = 17$ meV for both QD's. We finally determine the QD diameter ϕ which solves the variational problem for ξ and gives the measured energetic confinements E_1 and E_2. We find $\phi_1 = 15$ nm and $\phi_2 = 9$ nm corresponding to $\xi_1 = 4.7$ nm and $\xi_2 = 3.45$ nm (see Ref. 25).

To calculate the emission spectra, we proceed as in Ref. 17, considering that the probability W_p^q that the optical transition involves p phonons with energy $\hbar\omega_q$ is $W_p^q = [(n_{\mathbf{q}}+1)/n_{\mathbf{q}}]^{p/2} f(|M_q|^2)$ where $n_{\mathbf{q}} = (e^{\hbar\omega_{\mathbf{q}}/k_B T} - 1)^{-1}$ is the occupation Bose factor of the phonon state and f is given in Ref. 17. p is taken negative for anti-Stokes and positive for Stokes emission. For each phonon mode with energy $\hbar\omega_q$, each value of p gives rise to a line with height W_p^q on either side of the zero-phonon line.

For the calculation, we discretize the phonon dispersion with an energy step of the order of the zero-phonon linewidth. Each phonon-line contribution is then phenomenologically broadened by the zero-phonon line FWHM: at low temperature, we take the experimental FWHM shown in Fig. 2; for higher temperatures, we estimate the zero-phonon line FWHM by interpolating the low-temperature slope. Finally, to account for our experimental data, we only need to take $p = -2, \ldots, 2$.

Figure 4 presents the calculated spectra superimposed to the experimental ones. A nearly perfect agreement is found between experimental and theoretical curves for the exciton lines. At low temperature, the observed asymmetry of the phonon sidebands is well accounted for by our model. It can qualitatively be understood as follows. At low temperature, $n_q \ll 1$ so that the probability that an optical transition involves p ($p>0$) phonons is $W_p^q \propto [n_{\mathbf{q}} + 1/n_{\mathbf{q}}]^{p/2} \approx (1/n_q)^{p/2}$ for the low-energy sideband and is much larger than for the high-energy sideband ($W_p^q \propto n_q^{p/2}$).

In our model, ξ is the only parameter we change between QD1 and QD2. To understand how the QD size, through ξ, influences the exciton-phonon coupling, let us consider the Huang-Rhys factor $S_q = |M_q|^2/\hbar^2\omega_q^2$ characterizing the amplitude of the exciton-phonon coupling. S_q is plotted in Fig. 3(c) for the two QD's under study ($\xi_1 = 4.7$ nm, $\xi_2 = 3.45$ nm). We see that for QD2, S_q is larger than for QD1 and its maximum is obtained at higher q. In the second temperature range, where the measured linewidths are dominated by the phonon sidebands ($T > 25$ K), this explains why the QD2 line is broader than the QD1 line. Finally, S_q dramatically decreases when the QD size ϕ is around 40 nm ($\xi = 9.8$ nm) [see Fig. 3(c)]. This may explain why such phonon sidebands were not observed on larger QD's.[8]

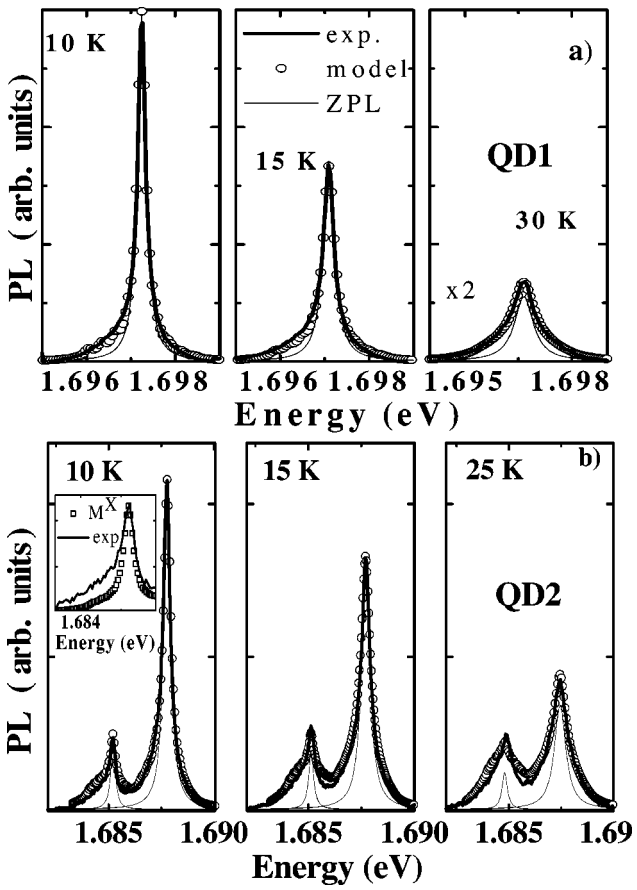

FIG. 4. Comparison between experimental emission spectra (thick lines) and calculated spectra (symbols) for various temperatures. The zero-phonon lines (ZPL) are shown in thin lines. (a): QD1. (b): QD2 with $M_{eff} = 2M_q^X$ for the biexciton line (inset: biexciton spectrum with $M_{eff} = M_q^X$).

It is worth to note that the FWHM of the zero-phonon line, which we introduce phenomenologically, cannot be accounted for by inelastic scattering with LO or LA phonons toward the two-dimensional(2D) quantum well. It may be due to the influence of the electrostatic environment induced by electron-hole pairs in the 2D quantum well.[26]

Finally, in literature, very different values can be found for D_c and D_v in GaAs [ranging from 6.5 eV to 1.5 eV for D_v and from -7 eV to -13.5 eV for D_c (Ref. 20)] However, phonon sidebands hardly contribute to the calculated spectra if one takes the smallest values of both $|D_v|$ and $|D_c|$ reported in literature. The theoretical analysis of our data gives a measurement of $|D_c - D_v|$ which is $|D_c - D_v| = 17 \pm 1$ eV.

We now extend our model to the biexciton case. The coupling matrix element is now given by

$$M_{\mathbf{q}}^{XX} = \sqrt{\frac{\hbar q}{2\rho u_s V}}\left(D_c\langle XX|e^{i\mathbf{q}\cdot\mathbf{r}_{\mathbf{e}_1}} + e^{i\mathbf{q}\cdot\mathbf{r}_{\mathbf{e}_2}}|XX\rangle - D_v\langle XX|e^{i\mathbf{q}\cdot\mathbf{r}_{\mathbf{h}_1}} + e^{i\mathbf{q}\cdot\mathbf{r}_{\mathbf{h}_2}}|XX\rangle\right). \quad (1)$$

We build the spatial part of the biexciton state $|XX\rangle$ as the symmetrized product of two exciton states: $|XX\rangle = (1/\sqrt{2}) \times (|X_{e_1,h_1}\rangle|X_{e_2,h_2}\rangle + |X_{e_1,h_2}\rangle|X_{e_2,h_1}\rangle)$, and neglect the Coulombic repulsion.[27] We then find $\langle XX|e^{i\mathbf{q}\cdot\mathbf{r}_{\mathbf{e}_1}}|XX\rangle = (\frac{1}{2}+\frac{1}{2}) \times \langle X|e^{i\mathbf{q}\cdot\mathbf{r}_{\mathbf{e}_1}}|X\rangle +$ (exchange terms) where the exchange terms are of the form $(\langle X_{e_1,h_1}|\langle X_{e_2,h_2}|)e^{i\mathbf{q}\cdot\mathbf{r}_{\mathbf{e}_1}}(|X_{e_1,h_2}\rangle|X_{e_2,h_1}\rangle)$, and represent an exchange of holes (or electrons) between the two excitons forming the biexciton, through the interaction with phonons. Finally, we find that $M_q^{XX} = 2M_q^X + M_q^{exchange}$.

To calculate the spectrum of the biexcitonic line, we have to take into account that the final state of the optical transition is an exciton state, also coupled to phonons. As a result, the probability that the optical transition between the biexciton state and the exciton state involves p phonons is $W_p^q = [(n_{\mathbf{q}}+1)/n_{\mathbf{q}}]^{p/2} f(|M_q^{eff}|^2)$, where $M_q^{eff} = M_q^{XX} - M_q^X$.[17] If the biexciton coupling to phonons were the same as the exciton coupling ($M_q^{eff} = 0$) then no phonon sidebands would be observed on the biexciton line. Here, we have $M_q^{eff} = M_q^X + M_q^{exchange}$: if exchange terms were negligible, the contribution of the phonon sidebands to the biexciton spectrum would be the same as for the exciton spectrum. The inset in Fig. 4(b) compares the biexciton calculated spectrum for $M_q^{eff} = M_q^X$ to the experimental one at $T = 10$ K. The calculated phonon sidebands are much weaker than the experimental ones. This shows that the exchange term increases significantly the contribution of the phonon sideband to the spectrum.

Figure 4 represents the biexciton calculated spectra, superimposed to the experimental ones, for $M_q^{eff} = 2M_q^X$ ($M_q^{exchange} = M_q^X$). We find a good agreement with the experiment at low temperature. This indicates that the biexciton is about three times as coupled to phonons as the exciton. It further suggests that the contribution of the exchange term to the phonon sidebands is of the same order as of the direct term for the exciton.

To conclude, we have observed the nonperturbative coupling to phonons for both exciton and biexciton states in single III-V QD's. Our model very well accounts for our experimental observations for QD's with different confinements. We show that the influence of confinement is an important clue to understand why phonon sidebands are sometimes observed and sometimes not. A simple extension of our model indicates that the stronger coupling between phonons and the biexciton state is probably due to exchange terms. Our findings make stronger the conviction that one cannot neglect the coupling between the QD and its environment for any states of the excitonic shell. Rather than considering this coupling as an undesired perturbation with respect to an ideal two-level system, we believe that complete understanding of these phenomena may lead to novel insights into quantum information based on QD's.

We would like to thank N. Bardou, L. Le Gratiet, and C. Dupuis for technological help and A. David, G. Bastard, and R. Ferreira for fruitful discussions. This work was partly supported by the ''Région Ile de France'' and the ''Conseil Général de l'Essonne.''

*Electronic address: pascale.senellart@lpn.cnrs.fr

[1] For a review, see *Single Quantum Dots, Topics of Applied Physics*, edited by P. Michler (Springer Verlag, Heidelberg, 2003).
[2] L.C. Andreani, G. Panzarini, and Jean-Michel Gérard, Phys. Rev. B **60**, 13 276 (1999).
[3] C. Santori, D. Fattal, J. Vuckovic, G.S. Solomon, and Y. Yamamoto, Nature (London) **419**, 594 (2002).
[4] J. Hours, S. Varoutsis, M. Gallart, J. Bloch, I. Robert-Philip, A. Cavanna, I. Abram, F. Laruelle, and J.M. Gérard, Appl. Phys. Lett. **82**, 2206 (2003).
[5] N.H. Bonadeo, J. Erland, D. Gammon, D. Park, D.S. Katzer, and D.G. Steel, Science **282**, 1473 (1998).
[6] X. Li, Y. Wu, D. Steel, D. Gammon, T.H. Stievater, D.S. Katzer, D. Park, C. Piermarocchi, and L.J. Sham, Science **301**, 809 (2003).
[7] U. Bockelmann and G. Bastard, Phys. Rev. B **42**, 8947 (1990).
[8] D. Gammon, E.S. Snow, B.V. Shanabrook, D.S. Katzer, and D. Park, Science **273**, 87 (1996).
[9] C. Kammerer, G. Cassabois, C. Voisin, M. Perrin, C. Delalande, Ph. Roussignol, and J.M. Gérard, Appl. Phys. Lett. **81**, 2737 (2002).
[10] M. Bayer and A. Forchel, Phys. Rev. B **65**, 041308 (2002).
[11] P. Borri, W. Langbein, S. Schneider, U. Woggon, R.L. Sellin, D. Ouyang, and D. Bimberg, Phys. Rev. Lett. **87**, 157401 (2001).
[12] S. Hameau, Y. Guldner, O. Verzelen, R. Ferreira, G. Bastard, J. Zeman, A. Lemaître, and J.M. Gérard, Phys. Rev. Lett. **83**, 4152 (1999).
[13] L. Besombes, K. Kheng, L. Marsal, and H. Mariette, Phys. Rev. B **63**, 155307 (2001).
[14] P. Palinginis and H. Wang, Appl. Phys. Lett. **78**, 1541 (2001).
[15] J. Hours *et al.* (unpublished).
[16] Charles Santori, Glenn S. Solomon, Matthew Pelton, and Yoshihisa Yamamoto, Phys. Rev. B **65**, 073310 (2002).
[17] C.B. Duke and G.D. Mahan, Phys. Rev. **139**, A1965 (1965).
[18] T. Takagahara, Phys. Rev. B **31**, 6552 (1985).
[19] S. Rudin, T.L. Reinecke, and B. Segall, Phys. Rev. B **42**, 11 218 (1999).
[20] I. Vurgaftman, J.R. Meyer, and L.R. Ram-Mohan, J. Appl. Phys. **89**, 5815 (2001).
[21] R. Scholz, J. Appl. Phys. **77**, 3219 (1995).
[22] I. Gorczyca, T. Suski, E. Litwin-Staszewska, L. Dmowski, J. Krupski, and B. Etienne, Phys. Rev. B **46**, 4328 (1992).
[23] L.C. Andreani and A. Pasquarello, Phys. Rev. B **42**, 8928 (1990).
[24] R.F. Kopf *et al.*, Appl. Phys. Lett. **58**, 631 (1991).
[25] $\xi^2 = \phi^2/[4\ln(m_X\phi^2 V_b/2\hbar^2)]$.
[26] C. Kammerer, C. Voisin, G. Cassabois, C. Delalande, Ph. Roussignol, F. Klopf, J.P. Reithmaier, A. Forchel, and J.M. Gérard, Phys. Rev. B **66**, 041306(R) (2002).
[27] O. Heller, Ph. Lelong, and G. Bastard, Phys. Rev. B **56**, 4702 (1997).